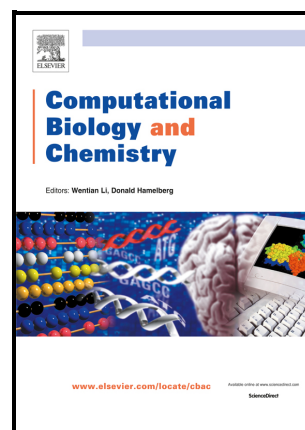


Relationship between Structural Properties and Biological Activity of (-)-Menthol and Some Menthyl Esters

Dilshod A. Mansurov, Alisher Kh. Khaitbaev, Khamid Kh. Khaitbaev, Khamza S. Toshov, Enrico Benassi



PII: S1476-9271(25)00017-9

DOI: <https://doi.org/10.1016/j.compbiolchem.2025.108357>

Reference: CBAC108357

To appear in: *Computational Biology and Chemistry*

Received date: 20 December 2024

Revised date: 12 January 2025

Accepted date: 15 January 2025

Please cite this article as: Dilshod A. Mansurov, Alisher Kh. Khaitbaev, Khamid Kh. Khaitbaev, Khamza S. Toshov and Enrico Benassi, Relationship between Structural Properties and Biological Activity of (-)-Menthol and Some Menthyl Esters, *Computational Biology and Chemistry*, (2025)
doi:<https://doi.org/10.1016/j.compbiolchem.2025.108357>

This is a PDF file of an article that has undergone enhancements after acceptance, such as the addition of a cover page and metadata, and formatting for readability, but it is not yet the definitive version of record. This version will undergo additional copyediting, typesetting and review before it is published in its final form, but we are providing this version to give early visibility of the article. Please note that, during the production process, errors may be discovered which could affect the content, and all legal disclaimers that apply to the journal pertain.

Relationship between Structural Properties and Biological Activity of (-)-Menthol and Some Menthyl Esters

Dilshod A. Mansurov^{1*}, Alisher Kh. Khaitbaev¹, Khamid Kh. Khaitbaev², Khamza S. Toshov¹ and Enrico Benassi^{3†*}

¹National University of Uzbekistan, Tashkent, 100057, Uzbekistan

²Institute of Bioorganic Chemistry named after O. Sodikov, Academy of Sciences of the Republic of Uzbekistan, Tashkent, 100057, Uzbekistan

³Department of Natural Sciences, Novosibirsk State University, Novosibirsk, 630090, Russia

* Corresponding Authors' E-Mail Addresses: mansurovdilshod789@gmail.com (DM) ; ebenassi3@gmail.com (EB)

† Present address: Department of Physics, Informatics and Mathematics, University of Modena and Reggio Emilia, Modena, 41125, Italy.

Abstract

Menthol is a naturally occurring cyclic terpene alcohol and is the major component of peppermint and corn mint essential oils extracted from *Mentha piperita L.* and *Mentha arvensis L.* Menthol and its derivatives are widely used in pharmaceutical, cosmetic and food industries. Among its eight isomers, (-)-menthol is the most effective one in terms of refreshing effect. While the invigorating property of (-)-menthol is generally known, this claim is based on a substantial amount of literature and experience. (-)-Menthol has consistently been reported to possess better cooling and refreshing qualities in comparison to its isomers, making it the preferred choice in a broad range of applications such as personal care products, pharmaceuticals and food additives. Additionally, the (-)-menthol molecular structure allows it to have a tighter fitting with the thermoreceptors in the skin and mucous membranes, and thus to provide a more intense cooling feeling. Thus, although others have similar properties to a degree, (-)-menthol is the best compared to all in its refreshing capacity. This study focuses on menthol and some of its esters, *viz.* menthyl acetate, propionate, butyrate, valerate and hexanoate, with the purpose of establish a connection between structural, electrostatic and electronic characteristics and biological effects. The mostly favoured interactions of the esters with biotargets were investigated at a molecular level, offering a plausible foundation for their bioactivity elucidation. This study is conducted at a quantum mechanical and molecular docking level. The results may be of possible usefulness in areas of applications, such as pharmacological research and drug.

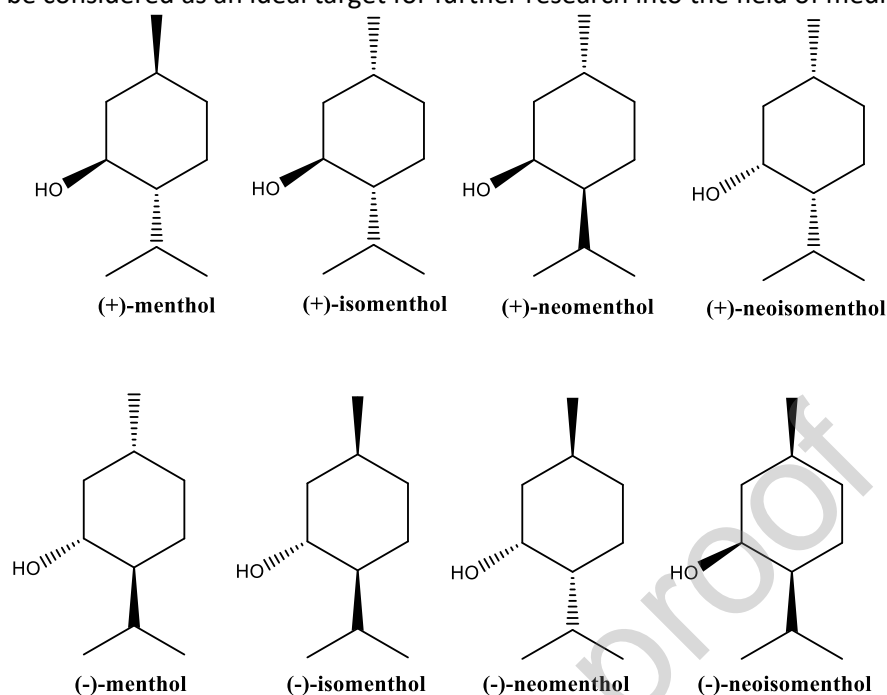
Keywords

Menthol ; Menthyl Esters ; Molecular Docking ; Density Functional Theory

1 Introduction

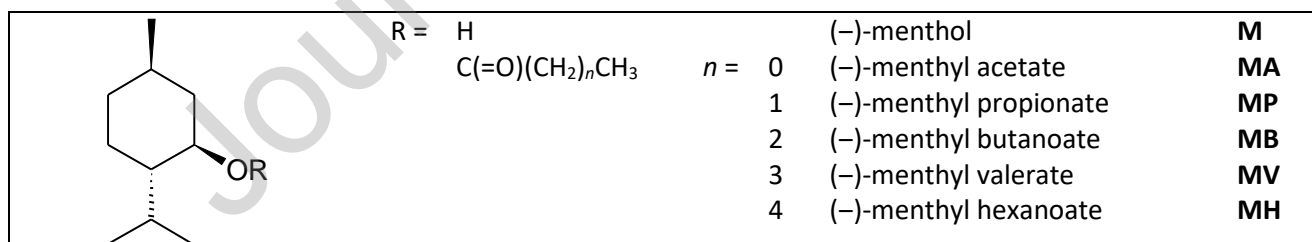
Menthol (2-isopropyl-5-methylcyclohexanol; molecular formula $C_{10}H_{20}O$; M), the major component in the essential oil of *Mentha piperita L.*, is a natural alcohol characterised by the presence of three asymmetrically substituted carbon atoms (stereocentres) and, thus, eight possible optical isomers exist, namely (+)- and (-)-menthol, (+)- and (-)-isomenthol, (+)- and (-)-neomenthol, (+)- and (-)-neoisomenthol (**Scheme 1**). M is known for its multiple biological functions **[1]** and is used as an ingredient possessing refreshing characteristics **[2-4]**, playing a role beyond being merely a sweetening or aromatic agent **[5]**. Recent researches focused on M's wide therapeutic applicability **[6,7]**, ranging from excellent antibacterial properties **[8,9]**, efficiency in eradicating a range of microorganisms **[10]**, an antioxidant function by preventing oxidative stress and consequently protecting cells **[11-13]** and demonstrating anti-aging effects at a cellular level **[20]**, and anti-inflammatory functions, which make it an important part of combating inflammation and related disorders **[14-16]**. The capability of M of modulating the immune system is another factor that enhances its position as one of the leading agents in the immune system's response regulation **[17]**. M was reported to show anti-cancer effects **[18]** and thus proposed as an adjunctive measure in the development of anti-cancer therapies **[19]**. M is also recommended for a plethora of other therapeutic conditions, such as, irritable bowel syndrome **[21]**, dyspepsia **[22]**, constipation and others functional gastrointestinal disorders, **[23]** as anti-depressant and anti-anxiety agent **[24,25]**, for the health of the oral **[26]** and urinary tract **[27]**, skin **[28]** and for wound healing **[29]**. A regular consumption of M might lead to memory improvement **[30]**. M is therefore a multi-functional agent, which is capable of

dealing with a broad spectrum of health-related issues. The in-depth analysis of the biological mechanisms of M allows it to be considered as an ideal target for further research into the field of medicine [31].



Scheme 1. The eight stereoisomers of menthol (M)

M derivatives and in particular its esters (MEs; Scheme 2) were found to indicate biological activity. For example, menthyl chloroacetate, menthyl dichloroacetate, menthyl cinnamate, menthone glyceryl acetalmethol thymol (b), α -terpineol and mugetanol exhibited greater mosquitocidal activity than menthol against *Cx. Quinquefasciatus* and *Ae. aegypti* [32]. The higher hydrolytic activity of three menthyl esters (*viz.* menthyl acetate MA, propionate MP and butyrate MB) was evaluated along with their enantiomeric excess, substrate conversion, and enantiomeric ratio, indicating MA as the most effective among the three. Additionally, the recombinant esterase from *E. coli* BL21 (pBSE) showed a superior enantioselectivity with this substrate. This highlights the suitability of MA as a substrate for efficient M production through enzymatic activity [33].



Scheme 2. Molecular structure of (-)-menthol (M) and its esters (MEs) investigated in this work. Adopted acronyms are also depicted.

In the current study, (-)-menthol (M) and a series of its esters, namely menthyl esters (MEs) - menthyl acetate, propionate, butyrate, valerate, and hexanoate - were studied using a computational approach. The main goal of this study was to identify the relationships between their structural, electrostatic, and electronic properties and their respective biological activities, thus providing a better insight into the relationship between molecular properties and bioactivity. Synergism of quantum chemical calculations and molecular docking simulations was applied in this pursuit. Quantum chemical calculations are performed to obtain molecular geometries, electronic distributions, and surface characteristics relevant for molecular reactivity and intermolecular interactions. The docking simulations carried out predict the binding affinity and detailed interaction pattern for these compounds with their target biomolecules, thus

rendering a comparison of potential biological activities. Such bifocal methodology can lead to a deep understanding of the physicochemical factors affecting the bioactivity of menthol derivatives and will help to systematically develop functional compounds with better characteristics. The binding interaction of M and MEs with two biologically relevant proteins, namely 7MHU, a sialidase from *Bacteroides acidifaciens*, and 3H1X, a phospholipase A2 (PLA2) enzyme from *Daboia russelii russelii* (Russell's viper), was calculated. 7MHU is described as the exo- α -sialidase, otherwise known as sialidase24 apo, that catalyses the hydrolysis of sialic acid residues from glycoconjugates. These enzymes are known to play fundamental roles in various biological events, such as cellular communication, pathogen recognition (pathogen-host interactions), immune response modulation, and cell signalling. Sialidases, such as 7MHU, are of therapeutic interest due to their involvement in diseases related to infections and glycosylation. The structure of the 7MHU protein has been experimentally determined using X-ray diffraction at a resolution of 2.00 Å [34]. 3H1X is a phospholipase A2 enzyme participating in the coagulation and inflammation pathways. PLA2 enzymes hydrolyze phospholipids, releasing arachidonic acid, which is a precursor to pro-inflammatory mediators like prostaglandins and leukotrienes. 3H1X protein was studied for its dual role in the inhibition of coagulation and inflammation [35]. It was co-crystallised with indomethacin, showing a new common ligand-binding site [36]. The structural characterisation was obtained by X-ray diffraction at the exquisite resolution of 1.40 Å [37]. Both proteins were chosen for this study based on the criteria of therapeutic implications, ligandability, and availability of experimentally determined high-resolution crystal structures. These characteristics ensure robust and reliable computational modelling, which now enables an exploration of the interactions between M (and MEs) and proteins in two distinct biological contexts, *viz.* sialidase-mediated processes and PLA2-associated inflammation and coagulation.

2 Materials and Methods

2.1 Quantum Chemical Calculations

Molecular geometry of M and MEs were fully optimised in the gas phase and in implicit ethanol solution, at Density Functional Theory (DFT) level (using B3LYP and M06-2X [38] hybrid functionals). In the cases of B3LYP functional, the D3 version of Grimme's empirical dispersion with Becke-Johnson damping was included. [39] The double- ζ 6-31+G** and the triple- ζ 6-311++G** [40] were used as a basis sets.

The optimised geometries were submitted to the calculation of the vibrational frequencies (in harmonic approximation) at the same levels of theory, to check whether the stationary points were genuine minima. The IR intensities and Raman activities along with the thermochemical quantities (at $T = 298.15$ K and $p = 1.00$ atm) were also computed.

The electrostatic properties of the optimised geometries were computed at DFT CAM-B3LYP[GD3BJ] [41] / Aug-CC-pVTZ [42] level within the CHELPG scheme. [43] This level of theory was shown to provide accurate values at a reasonable computational cost for organic molecules. [44]

Solvent effects were included using the SMD model. [45] Standard values of cavitation radii, dielectric properties and other technical parameters were used.

Using the triple- ζ 6-311++G** basis set, the same calculations were performed on EtOH and the amino acids interacting with M and MEs according to molecular docking simulations (*viz.*, ALA, ASP, CYS, GLY, ILE, LEU and LYS; *vide infra*), and on the complexes formed by these molecules and M and MEs.

For all calculations, the integration grid for the electronic density was set to 250 radial shells and 974 angular points for all the atomic species. The accuracy for the two-electron integrals and their derivatives was set to 10^{-14} a.u.. The self-consistent field (SCF) algorithm used was the quadratically convergent procedure designed by Bacskay, [46] a method that is acknowledged to be slower but more reliable than the regular SCF with DIIS extrapolation. The convergence criteria for the SCF were set to 10^{-12} for a root mean square (RMS) change in the density matrix and 10^{-10} for a maximum change in the density matrix. The convergence criteria for geometry optimizations were set to 2×10^{-6} a.u. for a maximum force, 1×10^{-6} a.u. for an RMS force, 6×10^{-6} a.u. for a maximum displacement and 4×10^{-6} a.u. for an RMS displacement.

All calculations were performed using the Gaussian G16.C01 package. [47]

2.2 PASS analysis

The molecular structures of the investigated compounds optimized at the DFT level were utilized as input for the Prediction of Activity Spectra for Substances (PASS) website (<https://way2drug.com/PassOnline>) to predict various biological activities, by means of the index Pa (predicted activity). Metabolite is an active compound if its Pa > 0.7, a moderately active compound if 0.5 < Pa < 0.7, or an inactive compound if Pa < 0.5 [48].

2.3 Swiss ADME

To assess the characteristics of M and the investigated MEs related to their pharmacokinetics properties (such as absorption, distribution, metabolism and excretion processes), we utilized the ADME tool developed by the Swiss Institute of Bioinformatics (SIB; www.swissadme.ch). For this evaluation, the Simplified Molecular Input Line Entry System (SMILES) strings representing each compound were input into the submission interface of Swiss ADME. This software computes parameters such as lipophilicity, hydrophilicity, solubility and permeability that play a role in understanding the compounds availability in biological systems and their potential interactions with cellular targets [49].

2.4 Molecular Docking

Docking simulations were carried out using the AutoDock Tools software [50] in order to investigate the potential interactions of M and MEs with two macromolecules associated to the PDB IDs 7MHU and 3H1X. The grid parameter file (GPF) defined the parameters needed for carrying out the docking simulations. For the 7MHU protein, the grid parameters were set with 92 grid points along the x-axis, 88 grid points along the y-axis, and 98 grid points along the z-axis. The coordinates for the center grid point were set to (22.211, 18.093, -0.229). The macromolecule file 7mhu.pdbqt was used for generating the grid maps. For the 3H1X protein, for example, the grid was made with 72 grid points on the x-axis, 74 grid points on the y-axis and 74 grid points along the z-axis. The middle grid point coordinate was taken as (-0.16, -16.355, -0.304). The macromolecule chosen was 3h1x.pdbqt from which files for the maps were designed. These parameters are critical in defining the search volume for molecular docking simulations and ensuring an accurate assessment of ligand-macromolecule interactions [51].

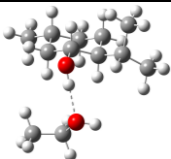
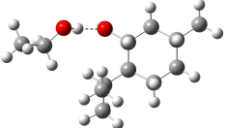
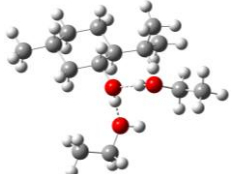
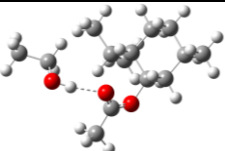
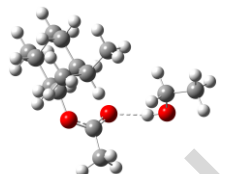
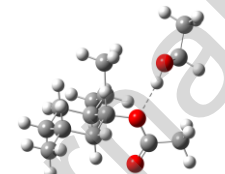
3 Results and Discussion

3.1 Molecular Structure

The molecular geometries of M and MEs were optimised at DFT level, using the hybrid functionals M06-2X and B3LYP combined with the double- ζ 6-31+G** and the triple- ζ 6-311++G** basis sets, both in gas phase and in EtOH solution. (The Cartesian Coordinates are reported in the ESI.) The main geometrical parameters (bond distances, bond angles and dihedral angles) are consistent to each other, independently of the chosen level of theory. Minor effects are attributed to the choice of the basis set and the solvation, which causes a slight elongation of a few bonds. The core structure of the selected molecules remains quite unchanged when the side moiety varies.

M and MA were employed to investigate the formation of hydrogen bonded complexes with EtOH, which may behave as a proton donor (D) or acceptor (A) when interacting with M, however only as D when interacting with MEs, which can interact with the hydroxyl proton of EtOH either *via* the carbonyl O atom or the etheric O atom (Table 1). The bond distance of hydrogen bonds (HBs) varies depending on the role played by EtOH and on the type of O atom the H atom bonds with. In cases of $[M \cdot (EtOH)_n]$ ($n = 1$ or 2) complexes, the HB is longer when EtOH molecule acts as A than D. In cases of $[MA \cdot EtOH]$ complexes, HBs formed between hydroxyl H atom of EtOH and the carbonyl O atom of the ME are shorter than those formed with the etheric O atom of the ME. From a thermodynamic point of view, the formation of these complexes is extremely favoured at room temperature. In particular, the formation of HB with MA seems to be more favoured than with M, because the HB with carbonyl O atoms and etheric O atoms are more stable than those with hydroxyl O atoms.

Table 1. Intermolecular complexes formed by M and MA with EtOH. The complex geometry, hydrogen bond length ($d(\text{HB})$), and the formation enthalpy (ΔH) and Gibbs free energy changes (ΔG) at $T = 298.15$ K are also depicted. Level of theory: DFT M06-2X / 6-311++G** (harmonic approximation; no scale factor). The complex was surrounded by a dielectric continuum (IEFPCM(SMD), solvent = EtOH).

	$d(\text{HB}) / \text{\AA}$	$\Delta H / (\text{kJ}\cdot\text{mol}^{-1})$	$\Delta G / (\text{kJ}\cdot\text{mol}^{-1})$
[M·EtOH]-(A)	 1.863	-734.6	-692.5
[M·EtOH]-(D)	 1.811	-736.4	-698.1
[M·(EtOH) ₂]	 1.791 (A) ; 1.765 (D)	-761.8	-685.7
[MA·EtOH]-(D1)	 1.860	-919.5	-884.0
[MA·EtOH]-(D2)	 1.859	-919.6	-884.4
[MA·EtOH]-(D3)	 1.903	-917.9	-879.3

3.2 Electrostatic Properties

The electrostatic properties of M and MEs were computed at DFT level, using the long-range corrected hybrid functional CAM-B3LYP combined with the triple- ζ Aug-CC-pVTZ basis set, both in gas phase and in EtOH solution. The Molecular Electrostatic Potential (MEP) represents a useful parameter to understand the electrostatic interactions between a substrate and the surrounding (*e.g.* solvent, enzyme, *etc.*). The MEP of M and MEs mapped on the total electron density shows the presence of a strongly positive area about the H atom of the OH group in M and a strongly negative area about the O atom both in M and MEs (Figure 1(a)). The hydrocarbon moieties are found slightly positive in MEP, with qualitatively similar distribution among MEs.

As expected, the values of electric dipole moment (μ) and its static isotropic polarizability ($\alpha_{(\text{iso})}$) increase in the series with the increase in size of the molecule (Table S1; Figure 1(b)-(c)). The presence of a polar environment (such as that determined by a polar solvent) enhances the values of the electrostatic parameters. In particular, the increase can be quantified as follows:

$$\mu(\text{EtOH}) = -2.550 + 2.9508 \mu(\text{gas}) \quad (R^2 = 0.9728), \quad (1)$$

$$\alpha_{(\text{iso})}(\text{EtOH}) = 1.23 + 1.3419 \alpha_{(\text{iso})}(\text{gas}) \quad (R^2 = 1). \quad (2)$$

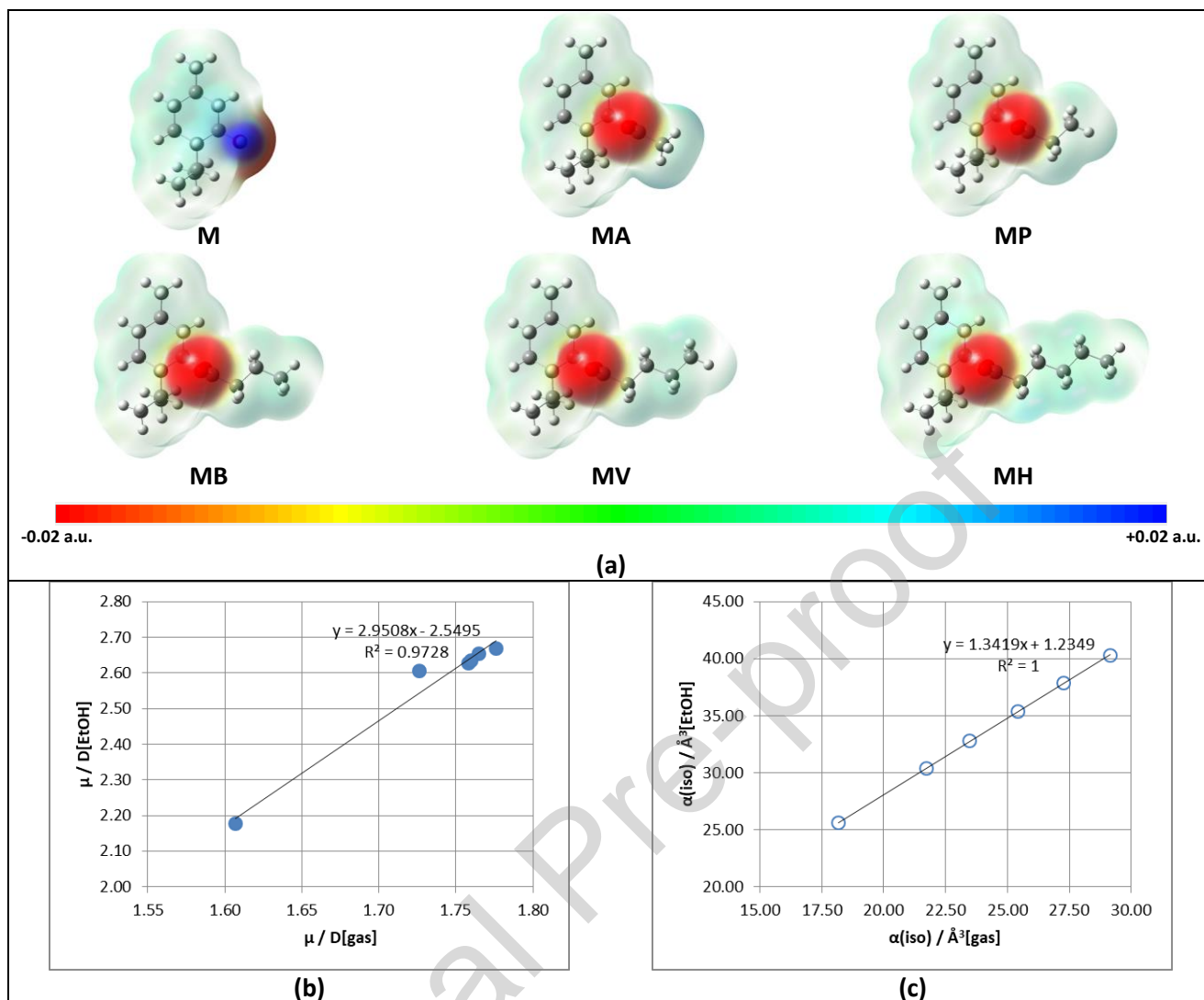


Figure 1. Electrostatic properties. (a) Molecular Electrostatic Potential (MEP) of M and MEs mapped on their total electron density (ρ). $|\text{Isolvalue}(\rho)| = 4 \times 10^{-4}$ a.u.. (b)-(c) Correlation between electric dipole moment (μ ; (b)) and static isotropic electric dipole polarizability ($\alpha(\text{iso})$; (c)) computed in the gas phase and in implicit EtOH. Level of theory: DFT CAM-B3LYP[GD3BJ] / Aug-CC-pVTZ.

The formation of HB complexes with molecules of EtOH increases the value of the electric dipole moment (*viz.*, $\mu = 4.61$ D, 4.70 D, 5.91 D, 5.13 D and 5.30 D for $[\text{M} \cdot \text{EtOH}]$ -(A), $[\text{M} \cdot \text{EtOH}]$ -(D), $[\text{M} \cdot (\text{EtOH})_2]$, $[\text{MA} \cdot \text{EtOH}]$ -(D1) and $[\text{MA} \cdot \text{EtOH}]$ -(D2), respectively), except for the complexes $[\text{MA} \cdot \text{EtOH}]$ -(D3) ($\mu = 1.08$ D).

Solubility of M and MEs in EtOH was evaluated at a QM level (Table S2). The reported values refer to the change in thermochemical parameters occurring when the molecule is optimised in the solution phase compared to the gas phase; these values therefore include the internal reorganisation energy. The values of ΔH and ΔG are negative, indicating that the solvation process is favoured. In the case of MEs, using values computed at DFT M06-2X / 6-311++G** (IEF-PCM(SMD)) level, ΔH linearly decreases with the number of C atoms of the side chain n , as follows:

$$\Delta H = -40.9 - 2.4971 n. \quad (R^2 = 0.9982) \quad (3)$$

On the other hand, ΔG does not show an evident trend, whose least value is obtained for MB. The PCM non-electrostatic term ($\Delta G_{(\text{PCM})}$) also show a linear decrease with n , *i.e.*:

$$\Delta G_{(\text{PCM})} = -4.0 - 1.8935 n. \quad (R^2 = 0.9914) \quad (4)$$

Calculations were repeated using the double- ζ 6-31+G** basis set, with very similar results; however, correlations were slightly worse than those identified using the triple- ζ 6-311++G** basis set.

3.3 Bioactivity and Molecular Docking

A comprehensive screening of Pa values for M and MEs as possible vasoprotectors, anti-inflammatory or antipyretic or antieczematic agents was obtained by PASS Online (Figure 2; numerical values are depicted in Table S3). These results predict pharmacological properties and bioactivities of the investigated compounds. M showed the highest values of Pa as a vasoprotective and antieczematic compound. Among the MEs, the longer the alkyl chain, the more effective the compound. On the other hand, MEs resulted to be more effective as anti-inflammatory (MB) and antipyretic (MP). M seems to be the least active as anti-inflammatory or antipyretic. However, the real effectiveness might be significantly different than that predicted by this method, depending on several factors, such as mechanisms of action, type of disease and individual response. This approach allowed these molecules to be considered as potentially bioactive [52]. The most important role of Pa (active) and Pi (inactive) is in providing the probabilities of first- and second-kind errors. The Pa values calculated for M and MEs indicate predicted activity probabilities for each of the molecules in the selected categories of therapeutic areas [53].

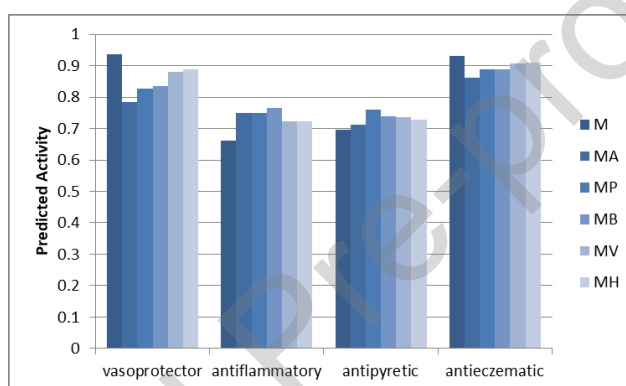


Figure 2. Predicted activity profiles of M and MEs.

Molar refractivity (A) and lipophilicity ($\text{Log } P_{O/W}$) were evaluated using different methods implemented in SWISS ADME (Table 2 and Table S4). Molar refractivity (A) is a parameter that describes the molecular size and polarizability of a molecule. Higher numbers are characteristic of larger and more polarizable structures whose attachment to biological targets may improve and permeability of membranes may be affected. This is helpful in predicting the degree of interaction a compound is likely to achieve with or across biological membranes.

Table 2. Thermodynamic properties (in $\text{kcal}\cdot\text{mol}^{-1}$), viz. Helmholtz free energy (A), Internal energy (U), Entropy (S), Final intermolecular energy (E_{int}), Total energy (E_{tot}), Electrostatic energy (E_{el}) and estimated inhibition constant (K_i). The values were computed using geometries and charges calculated at DFT M06-2X / 6-311++G** (in EtOH solution) level. (Results obtained using geometries and charges calculated at other levels of theory are depicted in Table S4.)

	A	U	E_{int}	E_{tot}	E_{el}	$K_i / \mu\text{M}$
M	-1370.13	-5.89	-6.62	-6.33	-0.29	38.27
MA	-1370.27	-6.03	-7.61	-7.40	-0.22	11.92
MP	-1369.95	-5.71	-7.60	-7.50	-0.09	20.16
MB	-1369.92	-5.69	-7.88	-7.75	-0.13	20.81
MV	-1369.66	-5.42	-8.00	-8.05	+0.05	28.03
MH	-1369.66	-5.42	-9.06	-9.02	-0.04	7.73

The Log P (where P indicates the partition coefficient, expressed as the ratio of a compound's concentration in a non-polar solvent, octanol, and a polar solvent, water) is a characteristic of molecules

that shows up as hydrophobicity or lipophilicity and this property governs both physics-chemistry and the biological processes [51]. Different philosophies of evaluating Log P are adopted in the literature [54-56], resulting in as many parameters computed by SWISS ADME. The values of A are proportional to the electric dipole polarizability, by definition, and thus its value increases with the molecular volume. Except for iLOGP, the other lipophilicity functions linearly correlate with A ($R^2 > 0.97$), especially XLOGP3 and WLOGP ($R^2 > 0.98$; Figure 3 and Table S5). As expected, MEs show the tendency of increasing in lipophilicity with the elongation of the alkyl chain (number of C atoms). However, some exception can be revealed. The value of iLOGP calculated for M is lower than that calculated for MA. Comparing the values calculated for MB and MV, we observe that $i\text{LOGP}(\text{MV}) < i\text{LOGP}(\text{MB})$ and $\text{XLOGP3}(\text{MV}) < \text{XLOGP3}(\text{MB})$. Considering MV and MH, $\text{WLOGP}(\text{MH}) < \text{WLOGP}(\text{MV})$ and $\text{MLOGP}(\text{MH}) < \text{MLOGP}(\text{MV})$.

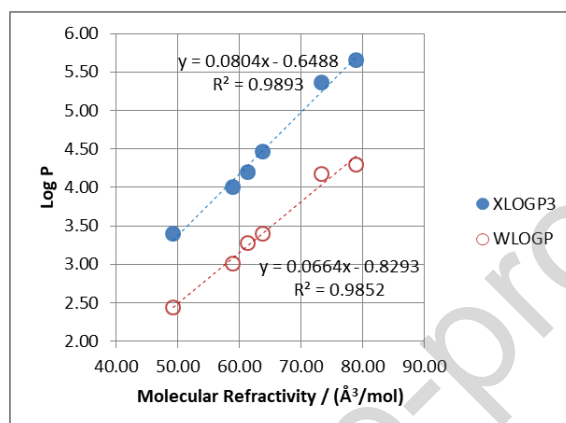


Figure 3. Correlation between values of LogP and molecular refractivity (A).

Solubility of M and MEs in water (S) were estimated with different approaches (*viz.*, ESOL, Ali and SILICOS-IT) using SWISS ADME (Tables S6). ESOL (Estimated Aqueous Solubility) model provides a solubility prediction for a drug compound, which is an important pharmacokinetics characteristic reflected as absorption, distribution, metabolism, and excretion (ADME) process in the body; a poorly or high solubility in water is commonly accompanied by improved bioavailability. Ali (Synthetic Accessibility Score) model determines the synthetic accessibility of the compound; in other words, it indicates how easy the synthesis of the compound in a laboratory is [57]. SILICOS-IT (Silicos In Silico) model predicts physicochemical properties, drug-likeness and bioactivities of the compound. In short, ESOL determines hydrophilic profiling, Ali shows synthetic opportunities, and SILICOS-IT offers a panel of predictions in connection with physicochemical properties, drug-likeness, or bioactivity indices [58, 59]. The results obtained for M and MEs with the three methods are consistent to each other. In comparison, Pastene-Burgos *et al.* utilized SwissADME and ADMET prediction services to evaluate ceanothanes derivatives, which were assessed for their potential as drug candidates for Alzheimer's disease (AD) treatment. Similar to our findings, they demonstrated high intestinal absorption prediction, acceptable Blood-Brain Barrier (BBB) permeability, and lipophilicity, which are essential for ADMET properties. Moreover, they assessed cardiotoxicity via hERG inhibition, and for M and MEs in the future investigations, we may also consider examining this criterion, although no issues were observed [60]. Upon linear regression, the values of water solubility calculated with the three methods are proportional to each other,

$$\text{Log } S (\text{ESOL}) = 1.2031 \text{ Log } S (\text{Ali}) - 0.2031 \quad (R^2 = 0.9617) \quad (5)$$

$$\text{Log } S (\text{ESOL}) = 1.3693 \text{ Log } S (\text{SILICOS-IT}) + 2.5628 \quad (R^2 = 0.9885) \quad (6)$$

$$\text{Log } S (\text{SILICOS-IT}) = 1.0871 \text{ Log } S (\text{Ali}) + 2.5522 \quad (R^2 = 0.9377) \quad (7)$$

As expected, MEs show a decrease in water solubility with the elongation of the alkyl chain; however, the poorest water solubility was attributed to MV, not MH. The solubility values show good linear trends with WLOGP and MLOGP,

Log S (ESOL) = -0.8156 WLOGP - 0.9826	($R^2 = 0.9799$)	(8)
Log S (ESOL) = -1.3385 MLOGP + 0.2623	($R^2 = 0.9483$)	(9)
Log S (Ali) = -0.9835 WLOGP - 1.3781	($R^2 = 0.9465$)	(10)
Log S (Ali) = -1.6348 MLOGP + 0.1859	($R^2 = 0.9398$)	(11)
Log S (SILICOS-IT) = -1.1327 WLOGP - 1.2711	($R^2 = 0.9962$)	(12)
Log S (SILICOS-IT) = -1.8685 MLOGP + 3.0292	($R^2 = 0.9741$)	(13)

Poor linear fittings were found for the other Log P cases ($R^2 < 0.9$). Eqs (8-13) indicate that the slope is always negative, in agreement with the chemical intuition.

The values of binding energies (ΔG_{bind}) of M and MEs with 3H1X and 7MHU protein were computed using geometries and charges optimised at four different quantum mechanical (QM) theoretical levels (Table 3 and S7). All of the computed ΔG_{bind} values are negative, indicating that the binding interactions between the ligands and the protein are energetically favourable. Moreover, different initial geometries and ESP charges give different results in ΔG_{bind} . The qualitative and quantitative picture varies depending on the set of initial geometries and ESP charges used. MH always presented the most stable binding affinity to 3H1X among all ligands studied, with ΔG_{bind} ranging from -6.67 kcal/mol to -6.92 kcal/mol.

However, no clear trend was observed with the previously calculated properties. [61]. Except for when parameters computed at B3LYP / 6-311++G** (EtOH) level are used, MH seems to form the most stable interactions also with the substrate 7MHU. With an increase in the number of alkyl chain, the binding interaction between the investigated molecules and 7MHU protein binding tends to increase. The length of the alkyl chain thus plays an essential role in defining the strength and stability of the complex formed between M and MEs and 7MHU. However, no evident quantitative trend was identified between ΔG_{bind} and the number of alkyl chain's C atoms. The binding energies for M and its esters range between -5.77 and -7.44 kcal/mol. Among the esters, MH (DFT B3LYP[GD3BJ] / 6-311++G** (in EtOH solution) displayed the strongest binding, with ΔG_{bind} values up to -7.44 kcal/mol. By comparison, M showed weaker binding affinities, with ΔG_{bind} values ranging from -5.62 to -6.00 kcal/mol, consistently with the loss of extended hydrophobic interactions provided by the ester chain. A similar trend was observed for MA, MP, MB, and MV, where the binding energies increased with the alkyl chain length, suggesting that hydrophobic and van der Waals interactions play a critical role in the binding of menthyl esters to the 3H1X protein. However, a clear quantitative relationship between the number of carbon atoms in the alkyl chain and ΔG_{bind} values was not established, which is consistent with the observations reported for the 7MHU protein. Comparison of the docking results of 3H1X and 7MHU indicated that compound MH showed the strongest binding affinity in both protein contexts, making it a promising candidate for further optimization and development in future studies. In respect to the 3H1X protein, MH registered binding energies up to -6.92 kcal/mol, which are slightly lower than those observed for the 7MHU protein (-7.44 kcal/mol). The observed differences in binding affinity could be attributed to differences in the binding pockets of the two proteins, which in turn modulate the nature and magnitude of interactions with the ligands. Compared with the pyrazolo pyrimidine derivatives, reported in the literature [62] with ΔG_{bind} in the range from -7.67 to -9.21 kcal/mol for potent compounds, M and MEs are less efficient binders. In fact, compound 8 of their study indicated a binding energy of -9.21 kcal/mol, while MH, the most potent binder within the panel of MEs, exhibited maximum $\Delta G_{bind} = -7.44$ kcal/mol when interacting with 7MHU and only -6.92 kcal/mol when reacting with 3H1X. This would suggest that, although natural compounds like M and its esters may exhibit weaker binding interactions compared to synthetic ligands, they still show moderate binding affinities. Such qualitative and quantitative variations in binding energies, brought about by the use of different QM levels and solvent conditions, emphasise the importance of computational parameters in molecular docking studies. Despite these differences, the global trend of increased binding affinity with respect to the length of the alkyl chain is consistently followed in both proteins, which definitely emphasizes the key role played by hydrophobic interactions in stabilising the ligand-protein complexes. Further experimental confirmations, such as inhibition assays or structural measurements, will be necessary to support these computational results and estimate the therapeutic potential of these substances.

Table 3. Binding energies (ΔG_{bind}) computed with 3H1X and 7MHU proteins, using geometries and charges optimised calculated at DFT M06-2X / 6-311++G** (in EtOH solution) level. (Results obtained using geometries and charges calculated at other levels of theory are depicted in Table S4.)

molecule	$\Delta G_{bind} / (\text{kcal}\cdot\text{mol}^{-1})$	
	3H1X	7MHU
M	-5.86	-5.78
MA	-6.33	-6.48
MP	-6.51	-6.72
MB	-6.69	-6.93
MV	-6.85	-7.18
MH	-6.92	-7.33

Other thermodynamic parameters, computed using different QM models' results as initial conditions, are reported in Table S4, including Helmholtz Free Energy (A), Internal Energy (U), Entropy (S), Final Intermolecular Energy (E_{int}), the sum of van der Waals energy, hydrogen bond (HB) energy and desolvation energy (E_{tot}), and Electrostatic Energy (E_{el}). Large negative values of A indicate a large stability of the system. It is conceivable that the M and MEs hold similar structures or have like comparable interactions in similar environments, resulting in similar values of A . Nearly identical results are a manifest the dependability and consistency of the employed numerical method. For all the levels of theory, the calculated values of A and U show excellent linear correlation ($R^2 > 0.997$), with values of the slope close to the unit (as expected from theory, $A = U - TS$) and positive values of intercepts, the latter indicating a constant, negative value of entropy. As for ΔG_{bind} , no obvious correlation was found between thermodynamic quantities computed at different levels of theory. The trend of a given property as a function of the number of C atoms of the side chain n may be different, depending on the level of theory. Results of $A = A(n)$ and $U = U(n)$ based on the geometries optimised at the DFT B3LYP[GD3BJ] / 6-311++G** level in the gas phase are oscillating; however, using the geometries optimised at the DFT M06-2X / 6-311++G** level in the gas phase, we found

$$A = 0.045 n^2 - 0.041 n - 1370.1 \quad (R^2 = 0.9959) \quad (14)$$

$$U = 0.046 n^2 - 0.045 n - 5.8386 \quad (R^2 = 0.9963) \quad (15)$$

For the other levels of theory, no evident trends between the values of $A = A(n)$ or $U = U(n)$ were identified. Except for geometries optimised at the DFT M06-2X / 6-311++G** level in EtOH, for which correlations were not satisfactory, with the other geometries, excellent linear fits were established between the values of E_{int} or E_{tot} and n ; for example, using the geometries optimised at the DFT M06-2X / 6-311++G** level in the gas phase, we found

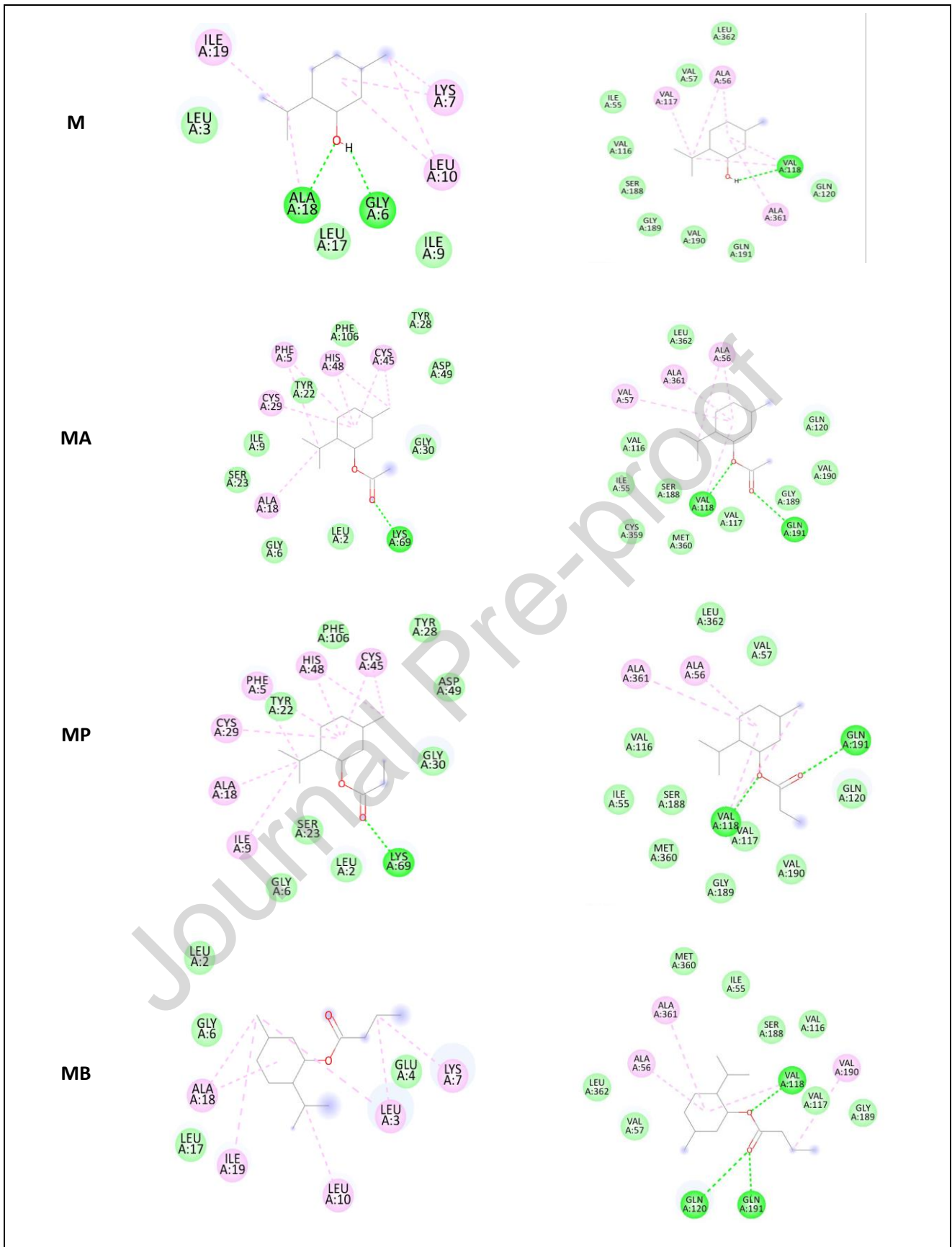
$$E_{int} = -0.396 n - 7.24 \quad (R^2 = 0.9625) \quad (16)$$

$$E_{tot} = -0.375 n - 7.20 \quad (R^2 = 0.9485) \quad (17)$$

No evident trends were identified for $E_{el} = E_{el}(n)$ or $K_i = K_i(n)$, with any molecular geometry.

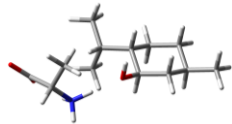
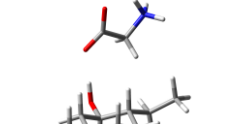
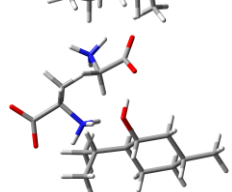
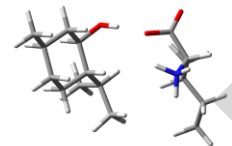
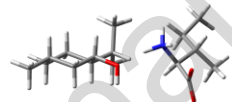
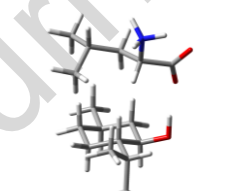
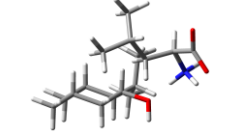
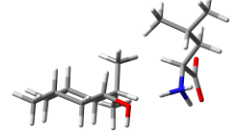
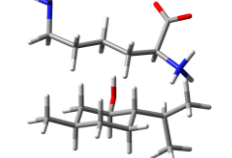
The MD simulations of M and MEs interacting with protein 3H1X and 7MHU provided insightful results about which amino acids are involved in the complex formation (Figure 4). The table highlights the binding interactions of six compounds with the target proteins, categorized into hydrophobic (alkyl), conventional hydrogen bonds, and van der Waals interactions.


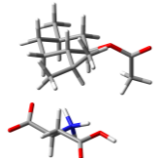
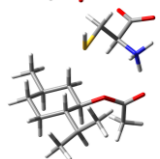
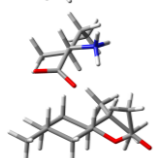
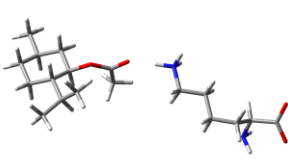
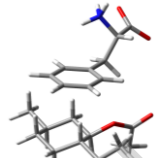
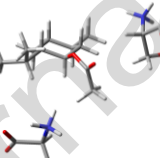
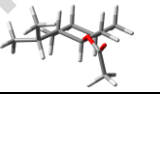
Compounds	3H1X	7MHU
-----------	------	------



less negative ΔG values than complexes with those formed by MA. The entropic factor is dominant in most of the investigated cases.

Table 4. Intermolecular complexes formed by M and MA with selected amino acids. The complex geometry, hydrogen bond length ($d(\text{HB})$, when HB forms), and the formation enthalpy (ΔH) and Gibbs free energy changes (ΔG) at $T = 298.15$ K are also depicted. Level of theory: DFT M06-2X / 6-311++G** (harmonic approximation; no scale factor). The complex was surrounded by a dielectric continuum (IEFPCM(SMD), solvent = EtOH).

		$d(\text{HB}) / \text{\AA}$	$\Delta H / (\text{kJ}\cdot\text{mol}^{-1})$	$\Delta G / (\text{kJ}\cdot\text{mol}^{-1})$
[M-ALA(A18)]		1.754	-5.3	-33.7
[M-GLY(A6)]		1.784	-0.7	-41.7
[M-GLY(A6)-ALA(A18)]		1.689(O) ; 1.666(N)	-47.3	-44.0
[M-ILE(A9)]		1.791	-3.8	-43.0
[M-ILE(A19)]		1.732	-11.5	-35.5
[M-LEU(A3)]		1.794	-6.2	-42.1
[M-LEU(A10)]		1.758	-6.4	-45.3
[M-LEU(A17)]		1.742	-11.4	-36.5
[M-LYS(A7)]		-	-12.1	-55.8

[MA-ALA(A18)]		-	43.1	-79.8
[MA-ASP(A49)]		-	27.9	-79.9
[MA-CYS(A29)]		1.769	-5.4	-46.6
[MA-ILE(A9)]		-	20.8	-70.9
[MA-LYS(A69)]		1.693	34.5	-88.1
[MA-PHE(A106)]		-	18.1	-63.5
[MA-SER(A23)]		-	36.5	-84.7
[MA-TYR(A22)]		-	16.2	-62.0

4 Conclusions

In this work, we evaluated properties and biological effectiveness of (-)-menthol (M) and some of its esters (MEs) obtained with linear chain alkyl carboxylic acids, *viz.* Menthyl Acetate, Menthyl Propionate, Menthyl Butyrate, Menthyl Valerate and Menthyl Hexanoate. A multifaceted approach encompassing various computational tools and platforms was adopted. Molecular geometries and electrostatic properties were calculated at the DFT level using two different hybrid exchange-correlation functionals (*viz.* B3LYP and M06-2X), combined with the 6-311++G** basis set, both in the gas phase and in implicit ethanol. Robust, quantitative relationships were identified between some solvation properties (ΔH and non-electrostatic $\Delta G_{(PCM)}$) and the number of C atoms of the alkyl ester chain.

Pa values for M and MEs as potential vasoprotective, anti-inflammatory, antipyretic or antieczematic drugs were calculated. Among the ligands, M showed the highest Pa values as vasoprotective and antieczematic drug. On the other hand, MEs showed higher activity as MB and MP. It was generally observed that the potency of MEs increased with an increase in the alkyl chain length, while M showed the least activity in terms of its anti-inflammatory or antipyretic activity. Its calculated physicochemical properties, including

molar refractivity, lipophilicity, and aqueous solubility indicate several quantitative relationships among them. Binding energies (ΔG_{bind}) of M and MEs to two target proteins, 7MHU and 3H1X, were calculated using molecular docking at the molecular dynamics level with geometries and ESP charges obtained using DFT. Quantitatively consistent trends in the ΔG_{bind} values were not obvious; however, all calculated binding energies were negative, indicative of favourable interactions upon binding. These results were also consistent with those obtained at a DFT level on intermolecular model complexes between M and MA and selected amino acids. Amongst the studied ligands, MH invariably showed the strongest binding affinity to both proteins. For example, in the case of 7MHU, it was found that the binding interactions generally improved with increasing alkyl chain length, which underlines the importance of hydrophobic interactions in stabilizing the ligand-protein complex. A similar trend was found with 3H1X, where again MH showed the most stable interactions. These findings suggest that the length of the alkyl chain is a critical determinant of the strength and stability of the complexes formed between the compounds studied here and their respective target proteins. Although M and MEs exhibit modest binding affinities in comparison with synthetic compounds, however they represent a promising molecular structure for further modifications and optimisation of their properties as multifunctional bioactive molecules. Biological experiments are currently on-going to verify the discoveries predicted in this work at a computational level.

Conflicts of interest

No potential conflict of interest was reported.

Acknowledgements

Computational resources were kindly provided by the HPCC at Nazarbayev University, Astana, Kazakhstan.

Authors' contribution

Dilshod A. Mansurov: data curation (docking); formal analysis; investigation; writing-review & editing.

Alisher Kh. Khaitbaev: supervision; editing.

Khamid Kh. Khaitbaev: conceptualisation; editing.

Khamza S. Toshov: visualisation; editing.

Enrico Benassi: conceptualisation; data curation (quantum mechanical calculations); formal analysis; investigation; methodology; project administration; writing the first draft; writing-review & editing.

References

- [1] A. Kazemi, A. Iraj, N. Esmaealzadeh, M. Salehi, and M. H. Hashempur "Peppermint and menthol: a review on their biochemistry, pharmacological activities, clinical applications, and safety considerations." *Crit. Rev. Food Sci. Nutr.* **2024**, *3*, 1-26.
- [2] J.A. Farco and O. Grundmann "Menthol--pharmacology of an important naturally medicinal "cool"." *Mini Rev. Med. Chem.* **2013**, *13*, 124-131.
- [3] T.R. Flood "Menthol use for performance in hot environments." *Curr. Sports Med. Rep.* **2018**, *17*, 135-139.
- [4] Ch.J. Stevens, M.L.R. Ross, and R.M. Vogel "Development of a "cooling" menthol energy gel for endurance athletes: effect of menthol concentration on acceptability and preferences." *Int. J. Sport Nutr. Exerc. Metab.* **2021**, *31*, 40-45.
- [5] A. Saint-Eve, I. Délérís, E. Aubin, E. Semon, G. Feron, J.-M. Rabillier, D. Ibarra, E. Guichard, and I. Souchon "Influence of composition (CO₂ and sugar) on aroma release and perception of mint-flavored carbonated beverages." *J. agricult. food chem.* **2009**, *57*, 5891-5898.
- [6] P. Mikaili, S. Mojaverrostami, M. Moloudizargari, and Sh. Aghajanshakeri "Pharmacological and therapeutic effects of Mentha Longifolia L. and its main constituent, menthol." *Ancient sci. life* **2013**, *33*, 131-138.
- [7] G.P.P. Kamatou, I. Vermaak, A.M. Viljoen, and B.M. Lawrence "Menthol: A simple monoterpene with remarkable biological properties." *Phytochem.* **2013**, *96*, 15-25.
- [8] V. Turcheniuk, V. Raks, R. Issa, I.R. Cooper, P.J. Cragg, R. Jijie, N. Dumitrascu, L.I. Mikhalovska, A. Barras, V. Zaitsev, R. Boukherroub, and S. Szunerits "Antimicrobial activity of menthol modified

- nanodiamond particles." *Diam. Relat. Mater.* **2015**, *57*, 2-8.
- [9] J. Wu, Y. Tianxiang, and X. Wang "Physicochemical and Anti-bacterial Properties of Novel Osthole-Menthol Eutectic System." *J. Sol. Chem.* **2022**, *51*, 1199-1208.
- [10] M. Mancuso "The antibacterial activity of *Mentha*." in *Herbs and spices* (Eds.: M. Akram and R. Sh. Ahmad), IntechOpen, **2020**.
- [11] A.L. Rozza, F.M. de Faria, A.R. Souza Brito, C.H. Pellizzon "The gastroprotective effect of menthol: involvement of anti-apoptotic, antioxidant and anti-inflammatory activities." *PLoS One* **2014**, *9*, e86686.
- [12] A.L. Rozza, F. Pereira Beserra, A.J. Vieira, E. Oliveira de Souza, C.A. Hussni, E.R. Monteiro Martinez, R.H. Nóbrega, and C.H. Pellizzon "The use of menthol in skin wound healing—Anti-inflammatory potential, antioxidant defense system stimulation and increased epithelialization." *Pharmaceutics* **2021**, *13*, 1902.
- [13] S.M. Hoseini, A.T. Mirghaed, B.A. Paray, S. Hossein Hoseinifar, and H. Van Doan "Effects of dietary menthol on growth performance and antioxidant, immunological and biochemical responses of rainbow trout (*Oncorhynchus mykiss*)." *Aquaculture* **2020**, *524*, 735260.
- [14] M.G. Zaia, T. di Orlando Cagnazzo, K.A. Feitosa, E.G. Soares, L.H. Faccioli, S.M. Allegretti, A. Afonso, and F. de Freitas Anibal "Anti-inflammatory properties of menthol and menthone in *Schistosoma mansoni* infection." *Front. Pharmacy* **2016**, *7*, 170.
- [15] F. Oliveira, E. Silva, A. Matias, J.M. Silva, R.L. Reis, and A.R.C. Duarte "Menthol-based deep eutectic systems as antimicrobial and anti-inflammatory agents for wound healing." *Eur. J. Pharmac. Sci.* **2023**, *182*, 106368.
- [16] S. Kehili, M. Nadjib Boukhatem, A. Belkadi, M. Amine Ferhat, and W.N. Setzer "Peppermint (*Mentha piperita* L.) essential oil as a potent anti-inflammatory, wound healing and anti-nociceptive drug." *Eur. J. Biol. Res.* **2020**, *10*, 132-149.
- [17] M. Cosentino, R. Bombelli, A. Conti, M.L. Colombo, A. Azzetti, A. Bergamaschi, F. Marino, and S. Lecchini "Antioxidant properties and in vitro immunomodulatory effects of peppermint (*Mentha piperita* L.) essential oils in human leukocytes." *J. Pharm. Sci. Res* **2009**, *1*, 33-43.
- [18] Y. Zhao, H. Pan, W. Liu, E. Liu, Y. Pang, H. Gao, Q. He, W. Liao, Y. Yao, J. Zeng, and J. Guo "Menthol: An underestimated anticancer agent." *Front. Pharmacol.* **2023**, *14*, 1148790.
- [19] K. Nagai, Sh. Fukuno, A. Omachi, S. Omotani, Ya. Hatsuda, M. Myotoku, and H. Konishi "Enhanced anti-cancer activity by menthol in HepG2 cells exposed to paclitaxel and vincristine: Possible involvement of CYP3A4 downregulation." *Drug Metab. Pers. Ther.* **2019**, *34*, 20180029.
- [20] R. Ram and M. Verma "HPLC and GC-MS Profiles for New Potential Sources of Anti-aging & Antioxidant Medicines in *Mentha Piperita* and *Ocimum Basilicum* var. *Thyrsi* Flora." *J. Diseases Med. Plants* **2023**, *9*, 60-71.
- [21] M. Egan, É.M. Connors, Z. Anwar, and J.J. Walsh "Nature's treatment for irritable bowel syndrome: studies on the isolation of (-)-menthol from peppermint oil and its conversion to (-)-menthyl acetate." *J. Chem. Educ.* **2015**, *92*, 1736-1740.
- [22] B.E. Lacy, W.D. Chey, M.S. Epstein, S.M. Shah, P. Corsino, L.R. Zeitzoff, and B.D. Cash "A novel duodenal-release formulation of caraway oil and L-menthol is a safe, effective and well tolerated therapy for functional dyspepsia." *BMC Gastroenterol.* **2022**, *22*, 1-9.
- [23] Q. You, L. Li, H. Chen, L. Chen, X. Chen, and Y. Liu "L-menthol for gastrointestinal endoscopy: a systematic review and meta-analysis." *Clin. Transl. Gastroenterol.* **2020**, *11*, e00252.
- [24] W. Wang, Yu. Jiang, E. Cai, B. Li, Y. Zhao, H. Zhu, L. Zhang, and Yu. Gao "L-menthol exhibits antidepressive-like effects mediated by the modification of 5-HTergic, GABAergic and DAergic systems." *Cognit. Neurodyn.* **2019**, *13*, 191-200.
- [25] Sh.-M. Zhu, R. Xue, Y.-F. Chen, Y. Zhang, J. Du, F.-Y. Luo, H. Ma, Y. Yang, R. Xu, J.-C. Li, Sh. Li, Ch.-W. Li, X. Gao, and Y.-Zh. Zhang "Antidepressant-like effects of L-menthol mediated by alleviating neuroinflammation and upregulating the BDNF/TrkB signaling pathway in subchronically lipopolysaccharide-exposed mice." *Brain Research* **2023**, *1816*, 148472.
- [26] T. Mahzoon, P. Koraei, O. Tavakol, M. Gholami, and A. Barfi "Effect of Limonene, Camphor and Menthol on Cariogenic Oral Pathogens." *PJMHS* **2022**, *16*, 706-709.

- [27] M. Shahid, M.Y. Lee, A. Yeon, E. Cho, V. Sairam, L. Valdiviez, S. You, and J. Kim "Menthol, a unique urinary volatile compound, is associated with chronic inflammation in interstitial cystitis." *Scient. Rep.* **2018**, *8*, 10859.
- [28] D.M. Over, N. Arjomandkhah, J.D. Beaumont, S. Goodall, and M.J. Barwood "Skin Application of Menthol Enhances Maximal Isometric Lifting Performance." *J. Strength Condit. Res.* **2023**, *37*, 564-573.
- [29] F. Oliveira, E. Silva, A. Matias, J.M. Silva, R.L. Reis, and A.R. C. Duarte "Menthol-based deep eutectic systems as antimicrobial and anti-inflammatory agents for wound healing." *Eur. J. Pharm. Sci.* **2023**, *182*, 106368.
- [30] N. Casares, M. Alfaro, M. Cuadrado-Tejedor, A. Lasarte-Cia, F. Navarro, I. Vivas, M. Espelosin, P. Cartas-Cejudo, J. Fernández-Irigoyen, E. Santamaría, A. García-Osta, and J.J. Lasarte "Improvement of cognitive function in wild-type and Alzheimer's disease mouse models by the immunomodulatory properties of menthol inhalation or by depletion of T regulatory cells." *Front. Immun.* **2023**, *14*, 1130044.
- [31] Sabzghabae, Ali Mohammad, et al. "Role of menthol in treatment of candidial napkin dermatitis." *World Journal of Pediatrics* 7 (2011): 167-170.
- [32] R. Samarasekera, I.S. Weerasinghe, and K.D.P. Hemalal "Insecticidal activity of menthol derivatives against mosquitoes." *Pest Manag. Sci.* **2008**, *64*, 290-295.
- [33] G.-W. Zheng, J. Pan, H.-L. Yu, M.-Th. Ngo-Thi, Ch.-X. Li, and J.-H. Xu "An efficient bioprocess for enzymatic production of L-menthol with high ratio of substrate to catalyst using whole cells of recombinant *E. coli*." *J. biotech.* **2010**, *150*, 108-114.
- [34] Kryshchak, Andriy, et al. "Computational models in the service of X-ray and cryo-electron microscopy structure determination." *Proteins: Structure, Function, and Bioinformatics* 89.12 (2021): 1633-1646.
- [35] Boyanovsky, Boris B., and Nancy R. Webb. "Biology of secretory phospholipase A 2." *Cardiovascular drugs and therapy* 23 (2009): 61-72.
- [36] Vinuchakkaravarthy, Thangaraj, et al. "Active compound from the leaves of *Vitex negundo* L. shows anti-inflammatory activity with evidence of inhibition for secretory phospholipase A2 through molecular docking." *Bioinformation* 7.4 (2011): 199.
- [37] Singh, Nagendra, et al. "Simultaneous inhibition of anti-coagulation and inflammation: crystal structure of phospholipase A2 complexed with indomethacin at 1.4 Å resolution reveals the presence of the new common ligand-binding site." *Journal of Molecular Recognition: An Interdisciplinary Journal* 22.6 (2009): 437-445.
- [38] Y. Zhao and D. Truhlar, "The M06 suite of density functionals for main group thermochemistry, thermochemical kinetics, noncovalent interactions, excited states, and transition elements: two new functionals and systematic testing of four M06-class functionals and 12 other functionals." *Theor. Chem. Acc.* **2007**, *120*, 215-241.
- [39] S. Grimme, S. Ehrlich, and L. Goerigk, "Effect of the damping function in dispersion corrected density functional theory." *J. Comput. Chem.* **2011**, *32*, 1456-1465.
- [40] (a) A. McLean and G. Chandler, "Contracted Gaussian basis sets for molecular calculations. I. Second row atoms, Z=11-18." *J. Chem. Phys.* **1980**, *72*, 5639-5648; (b) R. Krishnan, J. Binkley, R. Seeger, and J. Pople, "Self-consistent molecular orbital methods. XX. A basis set for correlated wave functions." *J. Chem. Phys.* **1980**, *72*, 650-654; (c) R. Binning and L. Curtiss, "Compact contracted basis sets for third-row atoms: Ga-Kr." *J. Comput. Chem.* **1990**, *11*, 1206-1216; (d) M. McGrath and L. Radom, "Extension of Gaussian-1(G1) theory to bromine-containing molecules." *J. Chem. Phys.* **1991**, *94*, 511-516; (e) L. Curtiss, M. McGrath, J. Blaudeau, N. Davis, R. Binning, and L. Radom, "Femtosecond bond breaking and charge dynamics in ultracharged amino acids." *J. Chem. Phys.* **1995**, *103*, 6104-6113.
- [41] T. Yanai, D. Tew, and N. Handy, "A new hybrid exchange-correlation functional using the Coulomb-attenuating method (CAM-B3LYP)." *Chem. Phys. Lett.* **2004**, *393*, 51-57.
- [42] (a) T. Dunning "Gaussian basis sets for use in correlated molecular calculations. I. The atoms boron

- through neon and hydrogen." *J. Chem. Phys.* **1989**, *90*, 1007-1023. (b) R. Kendall, T. Dunning and R. Harrison "Electron affinities of the first-row atoms revisited. Systematic basis sets and wave functions." *J. Chem. Phys.* **1992**, *96*, 6796-6806.
- [43] C. M. Breneman and K. B. Wiberg, "Determining atom-centered monopoles from molecular electrostatic potentials. The need for high sampling density in formamide conformational analysis." *J. Comput. Chem.* **1990**, *11*, 361-373.
- [44] E. Benassi, F. Egidi and V. Barone, "General strategy for computing nonlinear optical properties of large neutral and cationic organic chromophores in solution." *J. Phys. Chem. B* **2015**, *119*, 3155-3173.
- [45] A. V. Marenich, C. J. Cramer, and D. G. Truhlar, "Universal solvation model based on solute electron density and a continuum model of the solvent defined by the bulk dielectric constant and atomic surface tensions." *J. Phys. Chem. B* **2009**, *113*, 6378-6396.
- [46] G. B. Bacskay, "A Quadratically Convergent Hartree-Fock (QC-SCF) Method. Application to Closed Systems." *Chem. Phys.* **1981**, *61*, 385-404.
- [47] M. J. Frisch, G. W. Trucks, H. B. Schlegel, G. E. Scuseria, M. A. Robb, J. R. Cheeseman, G. Scalmani, V. Barone, G. A. Petersson and H. Nakatsuji, *et al.*, *Gaussian 16, Rev. C.01*, Gaussian Inc., Wallingford CT, **2019**.
- [48] D. A. Filimonov, A. A. Lagunin, T. A. Glorizova, A. V. Rudik, D. S. Druzhilovskii, P. V. Pogodin, and V. V. Poroikov "Prediction of the biological activity spectra of organic compounds using the PASS online web resource." *Chem. Heterocycl. Comp.* **2014**, *50*, 444-457.
- [49] D. Ranjith and C. Ravikumar "SwissADME predictions of pharmacokinetics and drug-likeness properties of small molecules present in *Ipomoea mauritiana* Jacq." *J. Pharmacogn. Phytochem.* **2019**, *8*, 2063-2073.
- [50] L. Ravi and K. Kannabiran "A handbook on protein-ligand docking tool: AutoDock 4." *Innov. J. Med. Sci.* **2016**, 28-33.
- [51] S.V. Giofrè, E. Napoli, N. Iraci, A. Speciale, F. Cimino, C. Muscarà, M.S. Molonia, G. Ruberto, and A. Saija "Interaction of selected terpenoids with two SARS-CoV-2 key therapeutic targets: An in-silico study through molecular docking and dynamics simulations." *Comp. Biol. Med.* **2021**, *134*, 104538.
- [52] G. Yalçın-Özkat "Computational studies with flavonoids and terpenoids as BRPF1 inhibitors: in silico biological activity prediction, molecular docking, molecular dynamics simulations, MM/PBSA calculations." *SAR QSAR Envir. Res.* **2022**, *33*, 533-550.
- [53] V. V. Poroikov, D. A. Filimonov, Yu. V. Borodina, A. A. Lagunin, and A. Kos "Robustness of biological activity spectra predicting by computer program PASS for noncongeneric sets of chemical compounds." *J. Chem. Inform. Comp. Sci.* **2000**, *40*, 1349-1355.
- [54] Yavuz, Sevtap Çağlar. "Quantum Chemical Computations, Molecular Docking, and ADMET Predictions of Cynarin." *Bitlis Eren Üniversitesi Fen Bilimleri Dergisi* **13.2**: 460-466.
- [55] M.T. Mahanthesh, D. Ranjith, Y. Raghavendra, R. Jyothi, G. Narappa, M.V. and Ravi "Swiss ADME prediction of phytochemicals present in *Butea monosperma* (Lam.) Taub." *J. Pharmacogn. Phytochem.* **2020**, *9*, 1799-1809.
- [56] B. Bakchi, A.D. Krishna, E. Sreecharan, V.B.J. Ganesh, M. Niharika, S. Maharshi, S.B. Puttagunta, D.K. Sigalapalli, R.R. Bhandare, and A.B. Shaik "An overview on applications of SwissADME web tool in the design and development of anticancer, antitubercular and antimicrobial agents: A medicinal chemist's perspective." *J. Mol. Struct.* **2022**, *1259*, 132712.
- [57] A. Ayar, M. Aksahin, S. Mesci, B. Yazgan, M. Gül, and T. Yıldırım "Antioxidant, cytotoxic activity and pharmacokinetic studies by Swiss ADME, Molinspiration, Osiris and DFT of PhTAD-substituted dihydropyrrole derivatives." *Curr. Comp.-aid. Drug Des.* **2022**, *18*, 52-63.
- [58] A. Azzam, M. Khaldun, El-S. Negim, and H.Y. Aboul-Enein "ADME studies of TUG-770 (a GPR-40 inhibitor agonist) for the treatment of type 2 diabetes using SwissADME predictor: In silico study." *J. Appl. Pharmac. Sci.* **2022**, *12*, 159-169.
- [59] Karabatak, Nesrin, Bahar Gök, and Yasemin Budama-kılinc. "Development of Nanoemulsion Formulation Containing Ylang Ylang Essential Oil for Topical Applications, Evaluation of In Vitro Cytotoxicity and ADMET Profile." *Journal of the Turkish Chemical Society Section A: Chemistry* **11.3**:

1181-1196.

- [60] A. Daina, O. Michielin, and V. Zoete "SwissADME: a free web tool to evaluate pharmacokinetics, drug-likeness and medicinal chemistry friendliness of small molecules." *Sci. rep.* **2017**, 7, 42717.
- [61] Kryshchak, Andriy, et al. "Computational models in the service of X-ray and cryo-electron microscopy structure determination." *Proteins: Structure, Function, and Bioinformatics* 89.12 (2021): 1633-1646.
- [62] M. Hussein, Sh. Hussein, and S.A. Ahmed "Reviewing of synthesis and computational studies of pyrazolo pyrimidine derivatives." *J. Chem. Rev.* **2019**, 1, 154-251.
- [63] F.M. Husain, I. Ahmad, M.S. Khan, E. Ahmad, Q. Tahseen, M.Sh. Khan, and N.A. Alshabib "Sub-MICs of *Mentha piperita* essential oil and menthol inhibits AHL mediated quorum sensing and biofilm of Gram-negative bacteria." *Front. Microbiol.* **2015**, 6, 420.
- [64] H. Sidhu, L.K. Gautam, and N. Capalash "Unraveling the molecular mechanism of l-menthol against cervical cancer based on network pharmacology, molecular docking and in vitro analysis." *Mol. Diver.* **2023**, 27, 323-340.

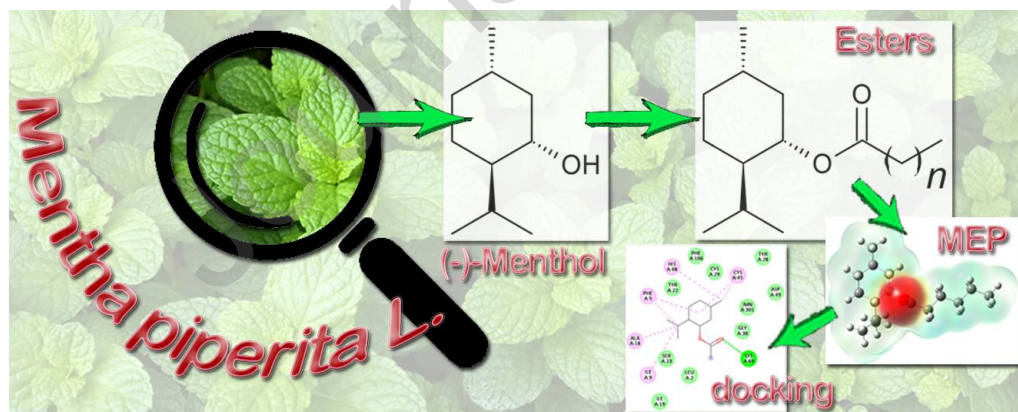
Authors' Statement

The authors declare no conflict of interest.

Declaration of interests

- The authors declare that they have no known competing financial interests or personal relationships that could have appeared to influence the work reported in this paper.
- The authors declare the following financial interests/personal relationships which may be considered as potential competing interests:

Graphical abstract



Highlights

- Quantitative relationships between side chain length and electrostatic properties
- Identification of biotargets of menthol and its esters.
- Quantitative relationships between structural properties and biological activity

Journal Pre-proof